CHAPTER IV
RESULTS AND DISCUSSION

4.1 Characterization of Vegetable oil

The vegetable oil used in this work was palm oil. Some properties, such as density, kinematic viscosity, free fatty acid content, and moisture content, were determined, as shown in Table 4.1. According to the Thai Industrial Standard (TIS 203-2520), an edible virgin oil is defined as an oil obtained by mechanical or thermal processes and may have been purified by washing, setting, filtering, or centrifuging. They are allowed to have an acid value not exceeding 4 mg KOH/g of oil and a maximum moisture content of 0.2%. Industrial vegetable oil is oil which is *not* edible, with an acid value of 10 mg KOH/g of oil and a moisture content higher than 0.5%. Using these criteria (Table 4.1), the palm oil used in this work can be classified as edible virgin oils.

Table 4.1 Properties of the palm oil

Properties	Palm oil
Density at 27°C (g/ml)	0.901
Kinematic Viscosity (cSt)	40.5155
Free fatty acid (%)	0.3579
Moisture Content (ppm)	452.8

The free fatty acid composition of palm oil was analyzed by a gas chromatograph, as shown as a chromatogram in Figure 4.1, and the composition of fatty acid in the palm oil is given in Table 4.2. The major fatty acid components for palm oil are oleic acid and palmitic acid. Based on these compositions, the molecular weight of the palm oil, about 850 g/mole, was calculated.

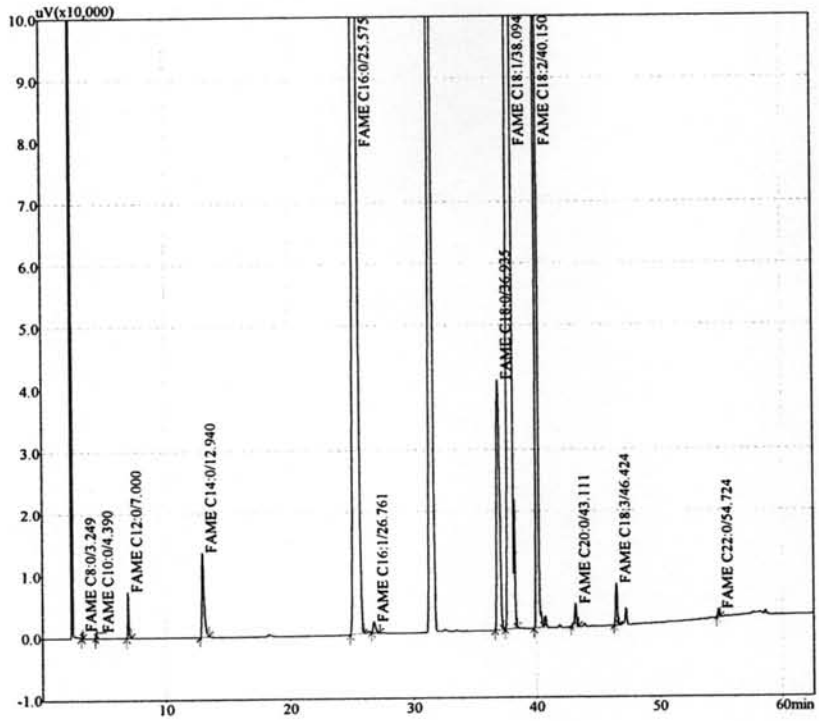

Figure 4.1 Chromatogram of the palm oil.

Table 4.2 Fatty acid composition of the palm oil

Fatty acid	Wt%
Caprylic acid (C8:0)	0.01
Capric acid (C10:0)	0.01
Lauric acid (C12:0)	0.20
Myristic acid (C14:0)	0.83
Palmitic acid (16:0)	40.29
Stearic acid (C18:0)	3.70
Oleic acid (C18:1)	43.73
Linoleic acid (C18:2)	10.64
Linolenic acid (C18:3)	0.19
Arachidic acid (C20:0)	0.30

4.2 Catalyst Characterization

4.2.1 X-ray Diffraction (XRD)

4.2.1.1 XRD patterns of fresh KOH/Al_2O_3 catalysts

The XRD patterns of KOH/Al_2O_3 with various wt% loadings of KOH are shown in Figure 4.2.

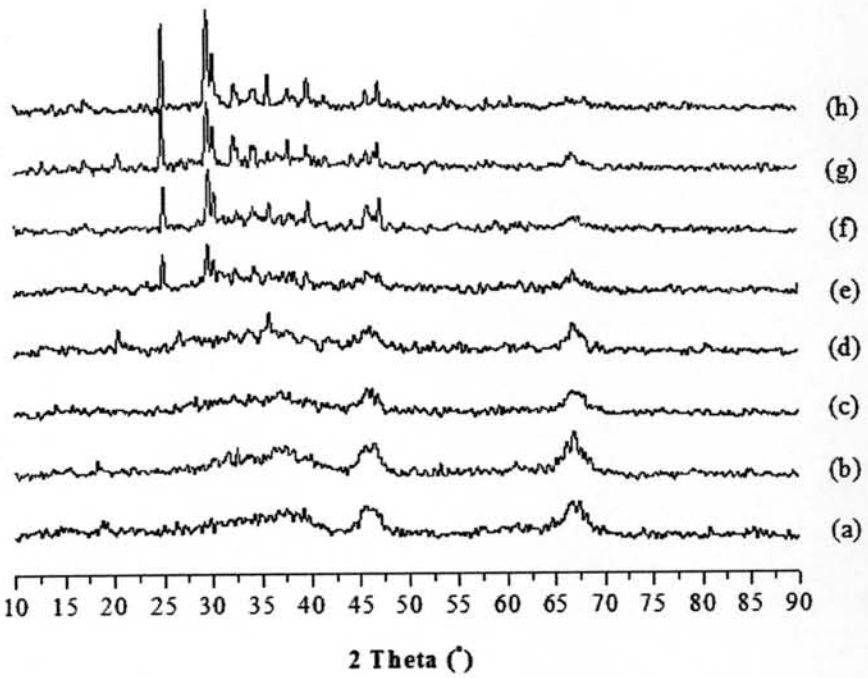

Figure 4.2 XRD patterns of the Al_2O_3 and KOH/Al_2O_3 catalysts: (a) Al_2O_3, (b) 5% KOH/Al_2O_3, (c) 10% KOH/Al_2O_3, (d) 15% KOH/Al_2O_3, (e) 20% KOH/Al_2O_3, (f) 25% KOH/Al_2O_3, (g) 30% KOH/Al_2O_3, and (h) 35% KOH/Al_2O_3.

The XRD patterns of fresh Al_2O_3 showed diffraction peaks at $2\theta = 20°$, 32°, 37°, 46° and 67°. When the loading amount of KOH was increased to 5% and 10%, the XRD patterns were almost the same with the typical pattern of Al_2O_3 because KOH can be well dispersed on the Al_2O_3 support in the form of a monolayer at a low loading of KOH. And if the loading amount of KOH is further increased to 15%, new phase of K_2O can be observed at $2\theta = 31°$, 39°, 51°, 55°, and 62° (Xie *et al.*, 2006). A new phase of K_2O can also be observed in 20% and 25%

KOH/Al_2O_3 at the same position. But if the loading amount of KOH is further increased over 30%, a new phase of a compound containing potassium and alumina elements could be observed at 2θ =17°, 23°, 25°, 29°, 30°, 31°, 34°, 36°, 38°, 40°, 44°, 46°, 47°, 48°, 51°, and 52° (JCPDS 00-019-0927). These results agree well with the result of KNO_3/Al_2O_3 reported by Xie *et al.* (2006). They explained that at low KOH loading, the XRD patterns are identical to that of Al_2O_3 because of the good dispersion of KOH on Al_2O_3. And when the KOH loading was increased to 15-25 wt%, the new phase of K_2O was observed. And if there is a further increase in the KOH loading to over 25 wt%, the new phase of Al-O-K compound could be observed.

4.2.1.2 XRD patterns of fresh KOH/NaY catalysts

The XRD patterns of KOH/NaY with various wt% loadings of KOH are shown in Figure 4.3.

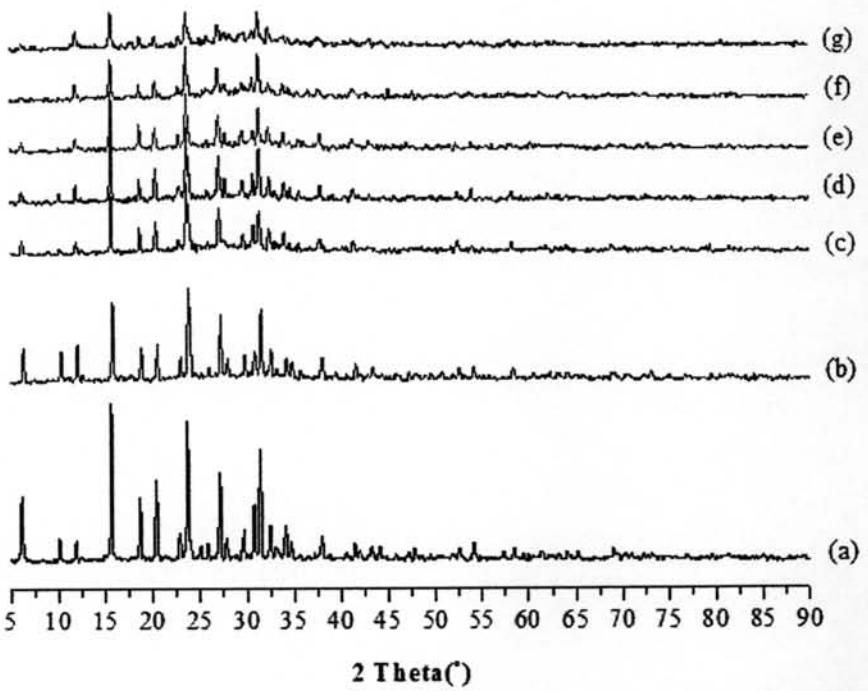

Figure 4.3 XRD patterns of the NaY and KOH/NaY catalysts: (a) NaY, (b) 7% KOH/NaY, (c) 8% KOH/NaY, (d) 9% KOH/NaY, (e) 10% KOH/NaY , (f) 13% KOH/NaY, and (g) 15% KOH/NaY.

The result shows that XRD patterns of all the KOH/NaY catalysts had the same XRD patterns as that of the NaY zeolite, and the intensity of the XRD patterns decreased when the loading amount of KOH was increased, showing diffraction peaks at 2θ = 6°, 10°, 12°, 13°, 14°, 16°, 17°, 18°, 20°, 21°, 23°, 24°, 25° , 26°, 27°, 28°, 29°, 30°, 31°, 32°, 33°, 34°, 35°, 36°, 38°, 40°, 41°, 42°, 43°, 44°, 45°, and 46° (JCPDS 00-039-1380). It was suggested that the loading amount between 7 and 15% had no significant effect on the crystalline structure. The result is in agreement with the result of KOH/NaX reported by Xie *et al.* They explained that the KOH modification could maintain the pore structure of zeolite, that is necessary for catalysis.

4.2.2 BET Surface Area Measurement

4.2.2.1 KOH/Al_2O_3 catalysts

The surface area pore volume and pore size of catalysts were determined by BET measurements. Table 4.3 shows the BET areas of both fresh and spent KOH/Al_2O_3 with various wt% loadings of KOH. The Al_2O_3 used as a support had a surface area of 208.48 m^2/g.

Table 4.3 Surface areas, pore volumes, and pore sizes of KOH/Al_2O_3 catalysts

Catalyst	Surface area (m^2/g)	Pore volume (cm^3/g)	Pore size (Å)
Fresh Al_2O_3	208.48	0.791	161.119
Fresh 5% KOH/Al_2O_3	228.80	0.272	21.550
Fresh 10% KOH/Al_2O_3	142.80	0.115	20.257
Fresh 15% KOH/Al_2O_3	97.50	0.089	21.920
Fresh 20% KOH/Al_2O_3	16.50	0.049	25.723
Fresh 25% KOH/Al_2O_3	7.68	0.050	25.512
Fresh 30% KOH/Al_2O_3	7.00	0.028	23.387
Fresh 35% KOH/Al_2O_3	3.71	0.012	10.692
Spent 25% KOH/Al_2O_3	47.00	0.044	21.550

The results showed that the surface area of fresh catalysts decreased when the loading amount of KOH was increased, whereas the surface area of the spent catalyst was higher than that of the fresh catalyst.

4.2.2.2 KOH/NaY catalysts

The surface areas and pore sizes of the catalysts were determined by BET measurement. Table 4.4 shows the BET areas of KOH/NaY with various wt% loadings of KOH. However, the surface area of the NaY support (738.01 m^2/g) is much higher than that of the Al_2O_3 support (208.48 m^2/g).

Table 4.4 Surface areas, pore volumes, and pore sizes of KOH/NaY catalysts

Catalyst	Surface area (m^2/g)	Pore volume (cm^3/g)	Pore size (Å)
Fresh NaY	738.01	1.221	6.176
Fresh 7% KOH/NaY	277.37	0.172	5.806
Fresh 8% KOH/NaY	205.12	0.093	6.718
Fresh 9% KOH/NaY	161.46	0.106	5.449
Fresh 10% KOH/NaY	35.59	0.118	80.764
Fresh 13% KOH/NaY	19.68	0.031	29.165
Fresh 15% KOH/NaY	13.81	0.002	9.789
Spent 10% KOH/NaY	14.08	0.040	20.461

Similarly, the surface area of the fresh KOH/NaY catalyst decreased when the loading amount of KOH was increased and the surface area of the spent catalyst was lower than that of the fresh catalyst.

4.2.3 Scanning Electron Microscopy with Energy Dispersive Spectrometry

4.2.3.1 KOH/Al_2O_3 catalysts

The morphologies of the catalysts and the results of the Energy Dispersive Spectrometry of both fresh and spent catalysts are presented in Figures 4.4 – 4.5.

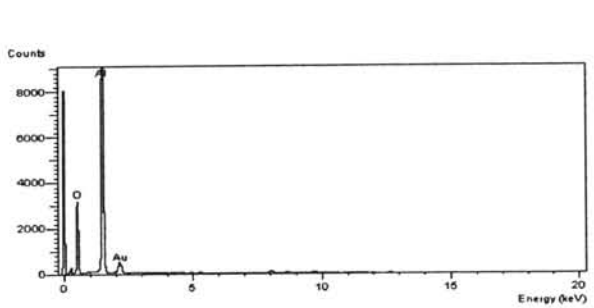

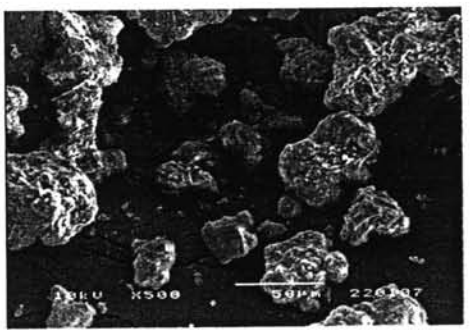

(a) Fresh Al_2O_3

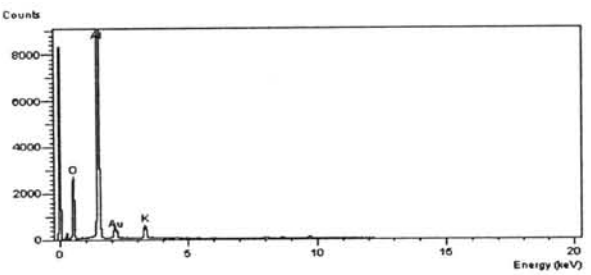

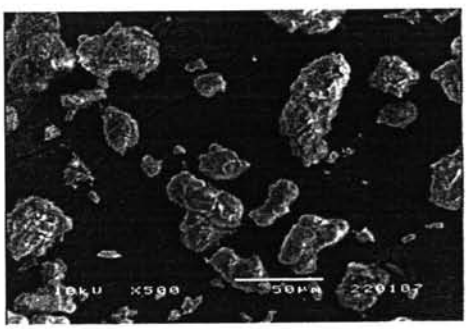

(b) Fresh 5% KOH/Al_2O_3

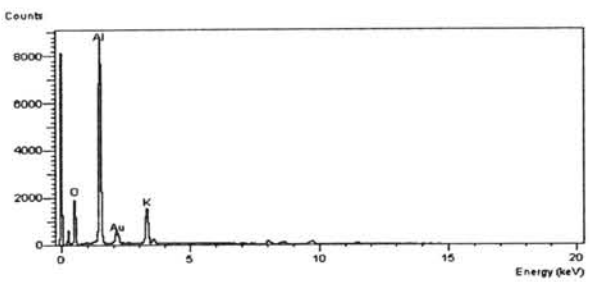

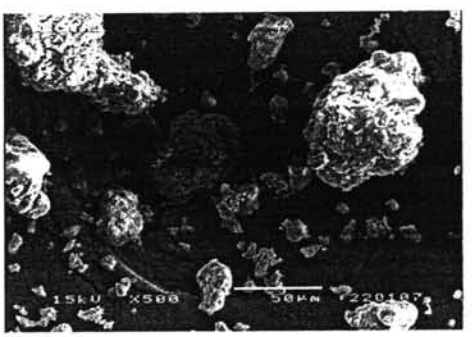

(c) Fresh 10% KOH/Al_2O_3

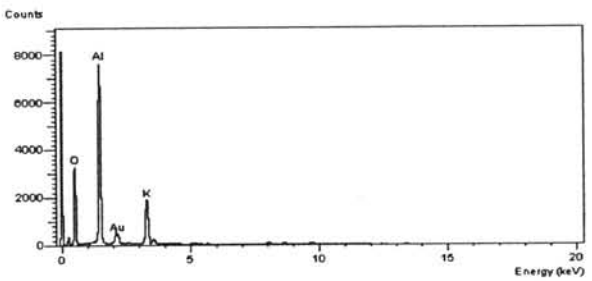

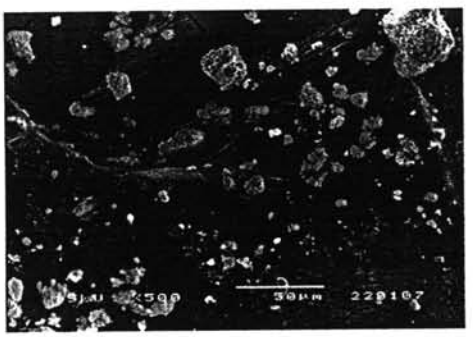

(d) Fresh 15% KOH/Al_2O_3

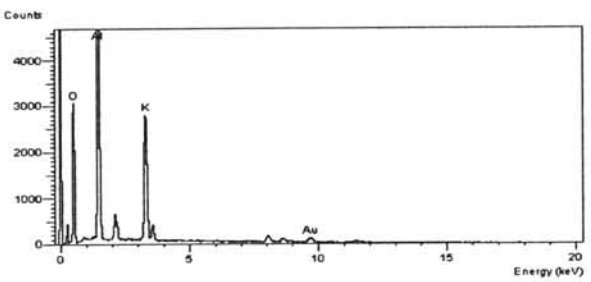

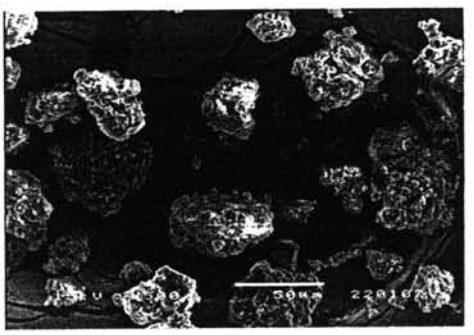

(e) Fresh 20% KOH/Al_2O_3

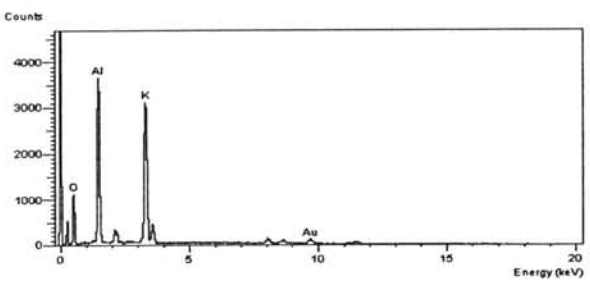

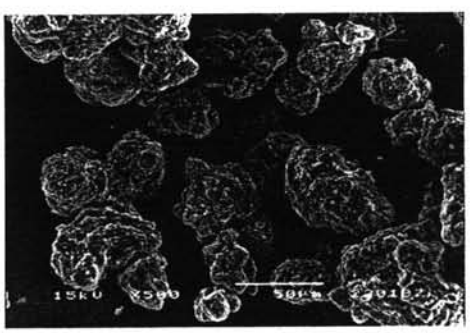

(f) Fresh 25% KOH/Al_2O_3

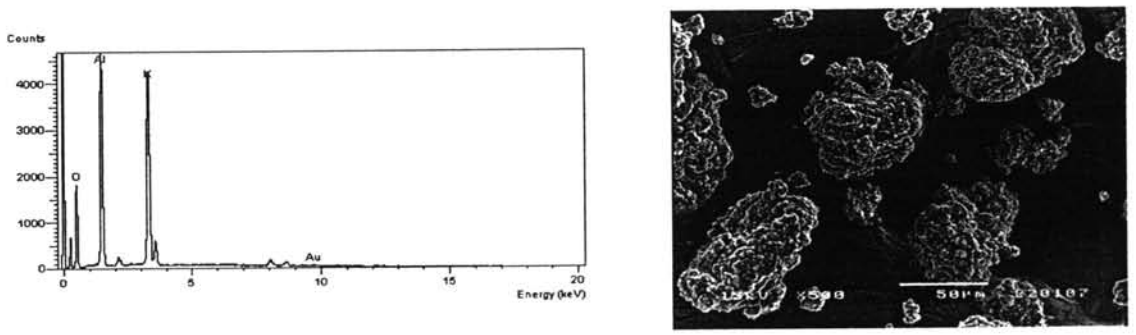

(g) Fresh 30% KOH/Al_2O_3

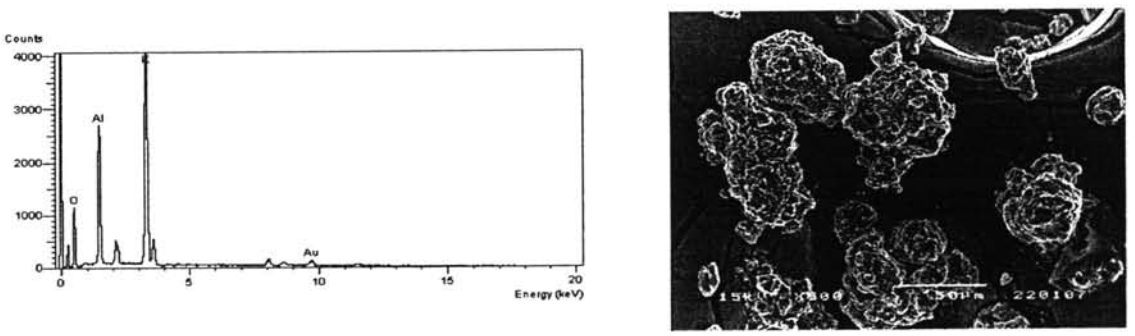

(h) Fresh 35% KOH/Al_2O_3

Figure 4.4 EDS-SEM of fresh KOH/Al_2O_3 catalysts.

The SEM results of the Al_2O_3 and KOH/Al_2O_3 showed crystals of 25-70 μm size, as shown in Figure 4.4 (a-h). Moreover, when the wt% loading of KOH was increased, the EDS could detect the increased quantity of potassium (K) element on the surface of catalyst. The quantity can be observed from the intensity of the potassium (K) element peak in the peak pattern. And the SEM results are consistent with the results from BET surface area measurements. The surface area of the fresh KOH/Al_2O_3 catalysts decreased when the wt% loading of KOH was increased because KOH has a good dispersion on the Al_2O_3 support at low wt% loading. At high loading of KOH, it forms large particles making the surface area of the prepared Al_2O_3 catalyst decrease. As can be seen, the KOH/Al_2O_3 catalysts have a

tendency to form large structures of catalyst when increasing the wt% loading of the KOH.

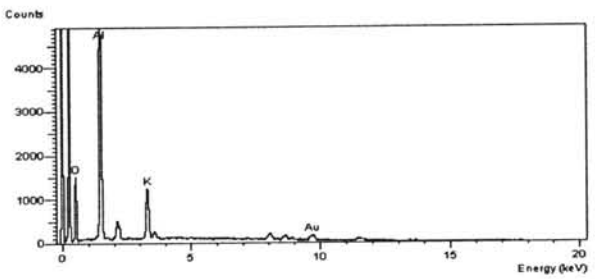

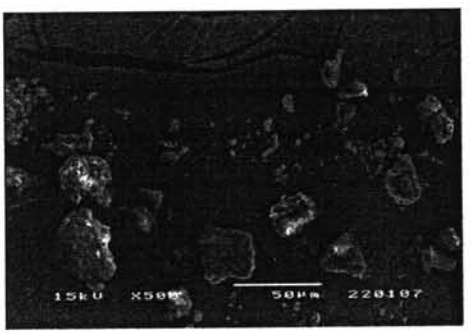

(a) Spent 15% KOH/Al_2O_3

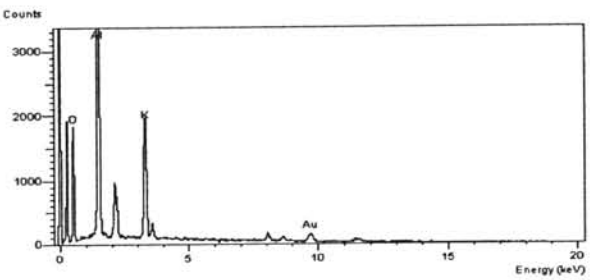

(b) Spent 20% KOH/Al_2O_3

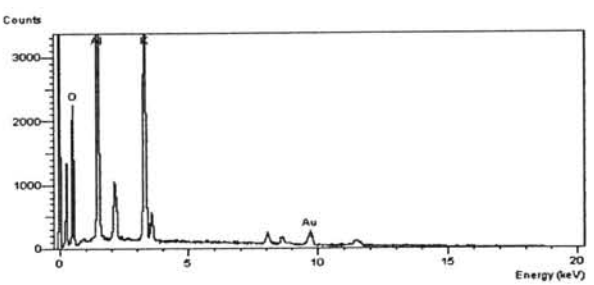

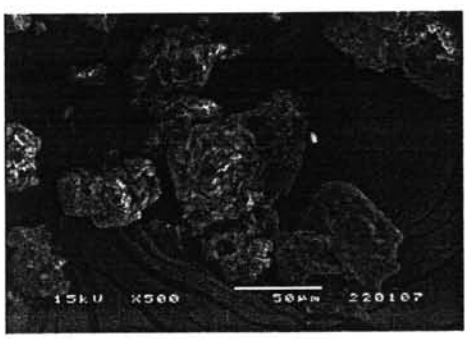

(c) Spent 25% KOH/Al_2O_3

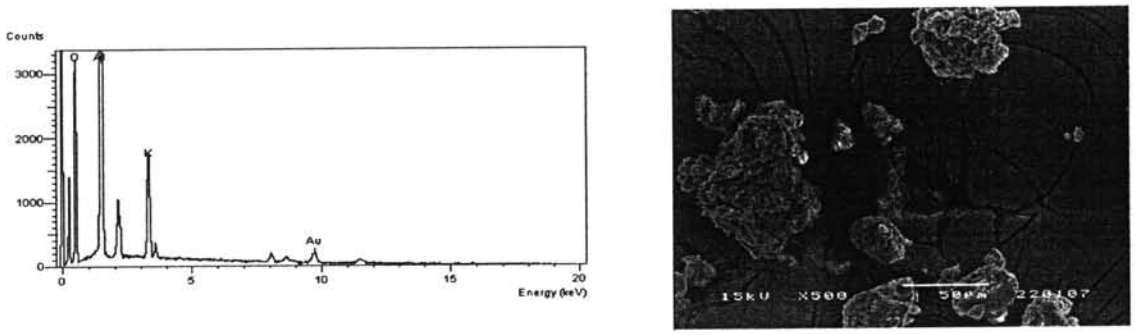

(d) Spent 30% KOH/Al_2O_3

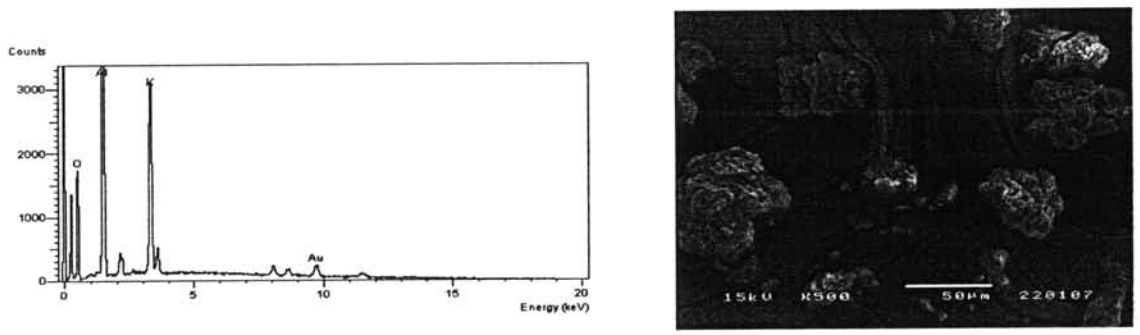

(d) Spent 35% KOH/Al_2O_3

Figure 4.5 EDS-SEM of spent KOH/Al_2O_3 catalysts.

In figures 4.4-4.5, the structures of the fresh and spent catalysts are compared. The results showed that the particles of the spent catalysts were smaller than those of the fresh catalysts. Therefore, the surface areas of the spent catalysts were higher than those of the fresh catalysts, as can be seen from the results of the BET surface area measurements. Moreover, the result of EDS showed that the quantity of the potassium (K) element contained on the surface of the spent catalyst is almost constant, indicating that the potassium (K) element on the surface of the Al_2O_3 was not consumed or leached when the reaction took place.

4.2.3.2 KOH/NaY catalysts

The morphology and the results of the Energy Dispersive Spectrometry of the fresh and spent catalysts are presented in Figures 4.6-4.7.

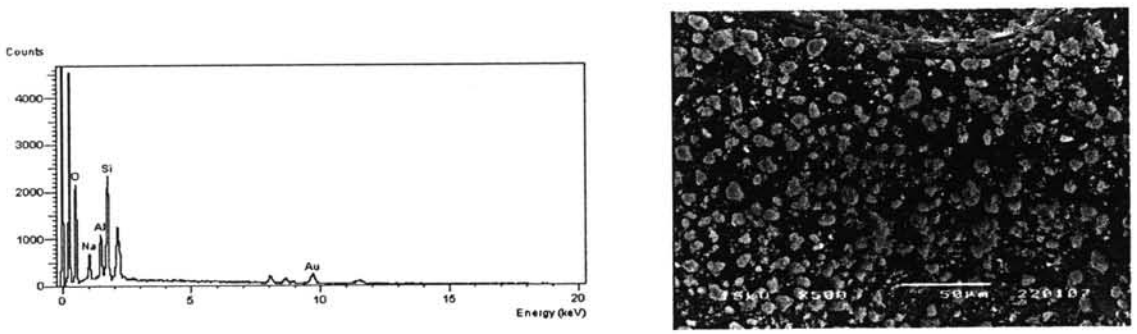

(a) Fresh NaY

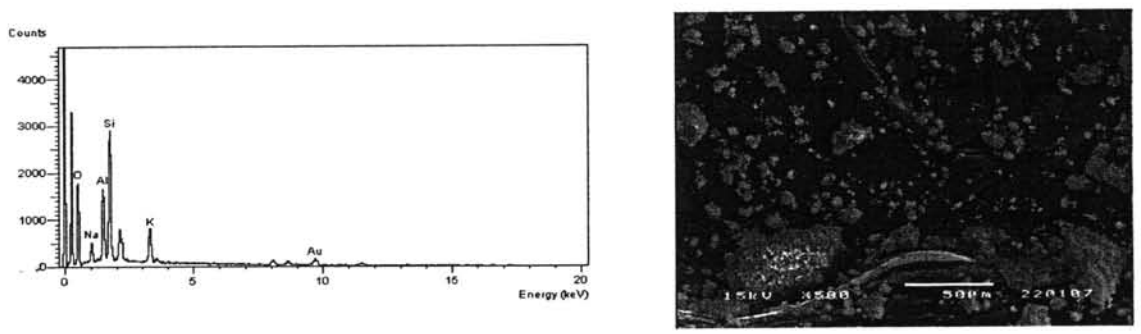

(b) Fresh 7% KOH/NaY

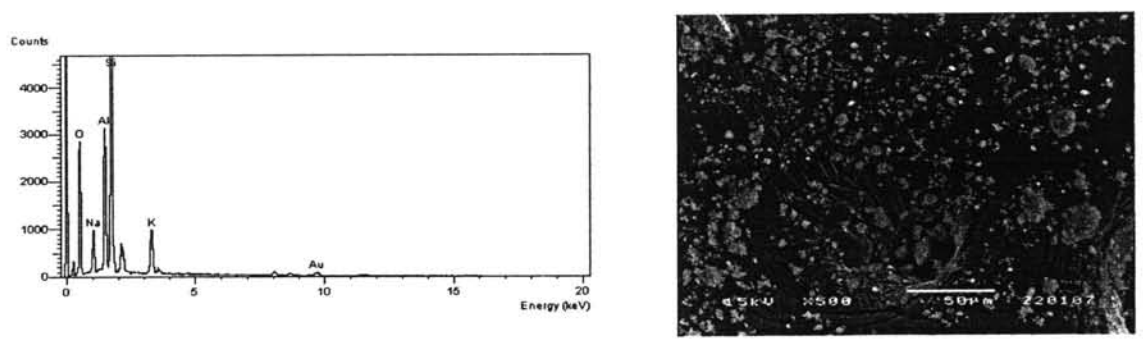

(c) Fresh 8% KOH/NaY

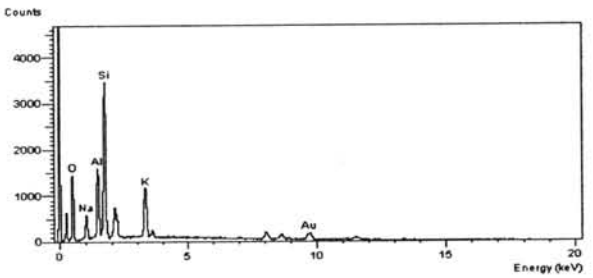

(d) Fresh 9% KOH/NaY

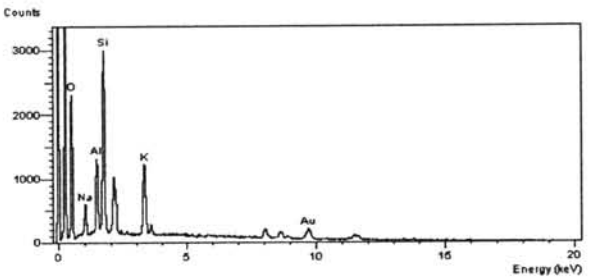

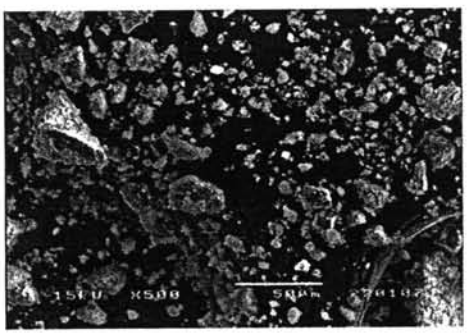

(e) Fresh 10% KOH/NaY

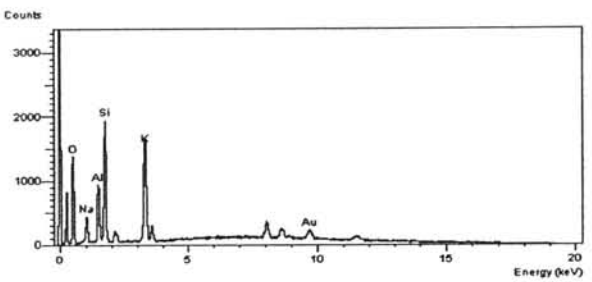

(f) Fresh 13% KOH/NaY

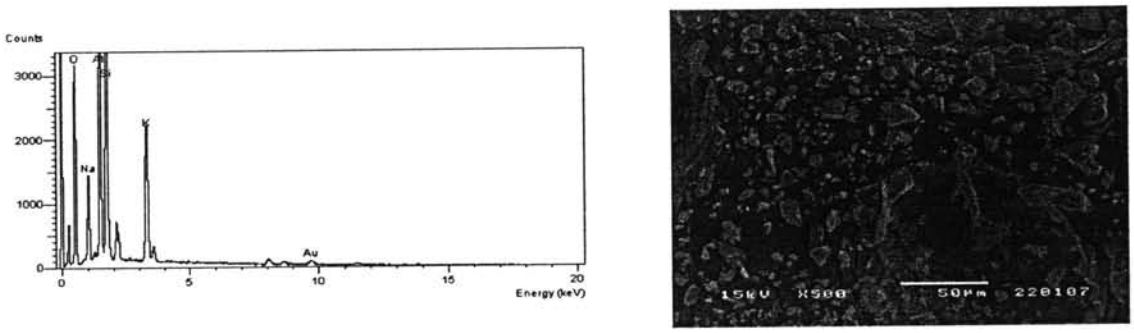

(g) Fresh 15% KOH/NaY

Figure 4.6 EDS-SEM of fresh KOH/NaY catalysts.

The SEM results of NaY and KOH/NaY showed crystals of 5-40 μm size, as seen in Figure 4.6 (a-g). Moreover when the wt% loading of KOH was increased, the EDS detected the increased quantity of potassium (K) element on the surface of the catalyst. The quantity can be observed from the intensity of the potassium (K) element peak. The EDS results can be used to describe the results from the BET surface area measurement. The surface area of fresh KOH/NaY catalysts were decreased when the wt% loading of KOH was increased because the KOH has a good dispersion on the NaY supported at low wt.% loading, but further increasing of KOH will form large particles, therefore making the surface area of the prepared NaY catalyst decrease. The results from the SEM capture show that the KOH/NaY catalysts have tendency to from large structures of the catalyst when increasing the wt% loading of the KOH.

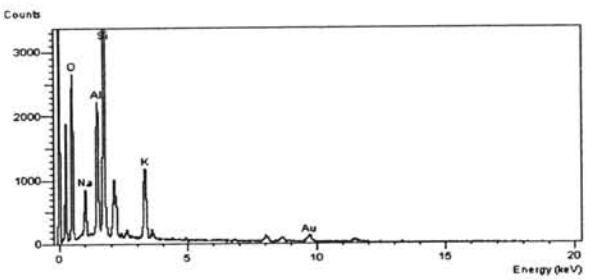

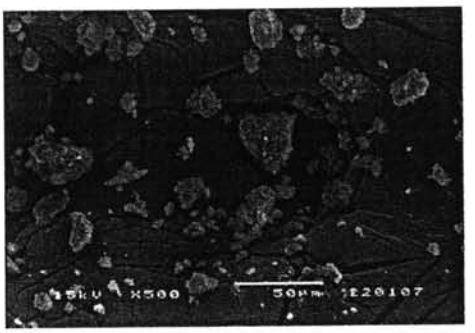

(a) Spent 8% KOH/NaY

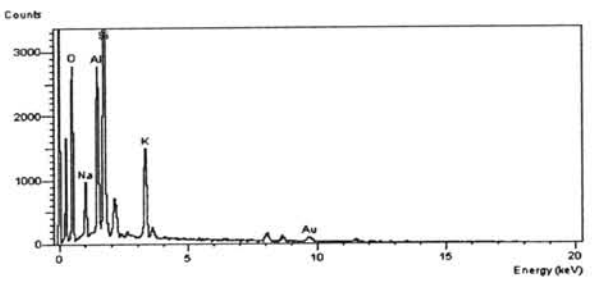

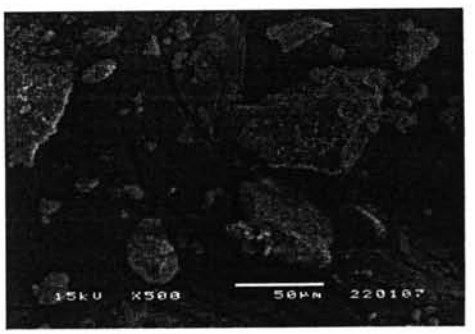

(b) Spent 9% KOH/NaY

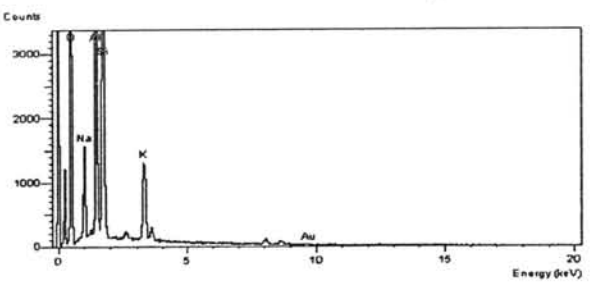

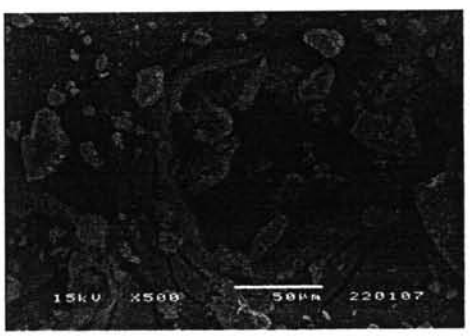

(c) Spent 10% KOH/NaY

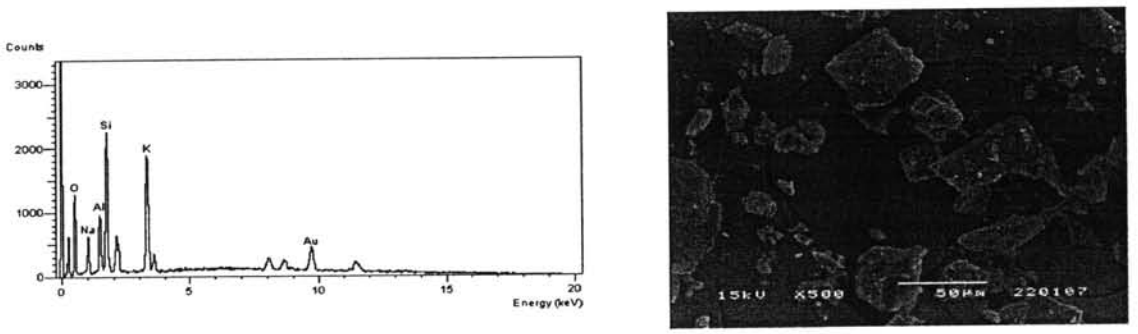

(d) Spent 13% KOH/NaY

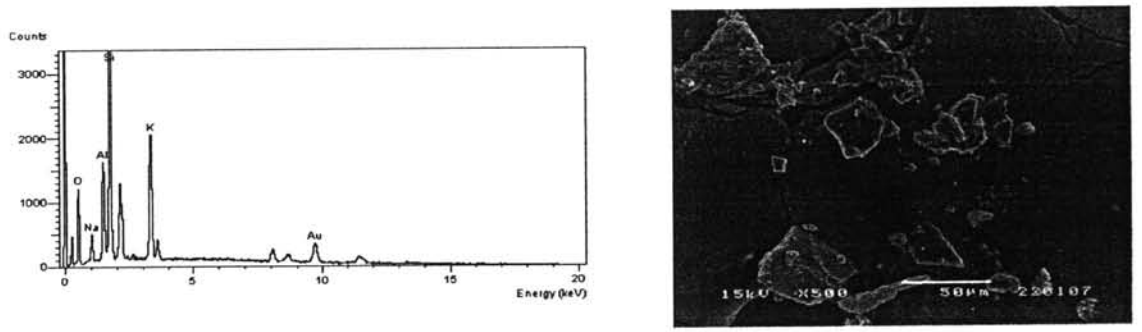

(e) Spent 15% KOH/NaY

Figure 4.7 EDS-SEM of spent KOH/NaY catalysts.

In figures 4.6-4.7, the structures of the fresh and spent catalysts are compared. The results show that the particles of the spent catalysts were bigger than those of the fresh catalysts. Therefore the surface areas of the spent catalysts were less than those of the fresh catalysts, as confirmed by BET surface area measurements. Moreover, the EDS results show that the quantity of the potassium (K) element on the surface of the spent catalyst is almost constant.

4.2.4 Temperature Program Desorption (TPD)

4.2.4.1 KOH/Al_2O_3 catalysts

The TPD profiles of desorbed CO_2 on Al_2O_3 and KOH/Al_2O_3 are shown in Figure 4.8.

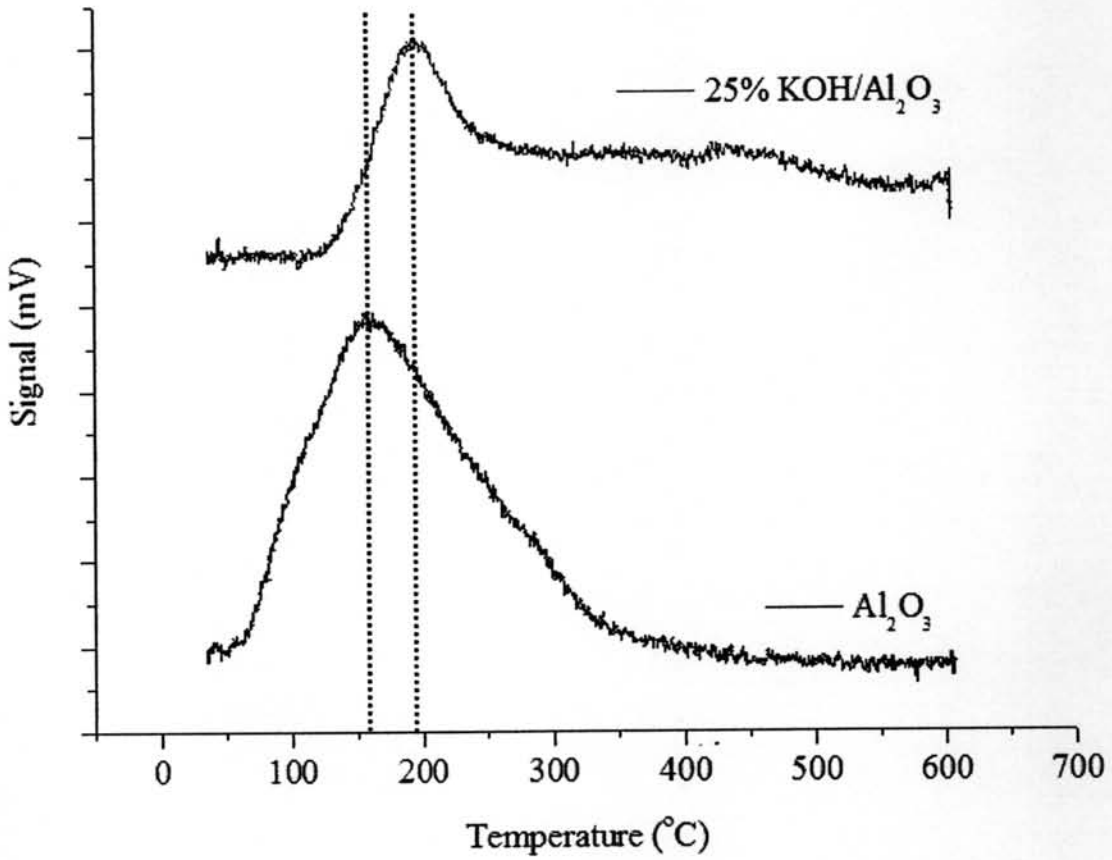

Figure 4.8 TPD profiles of CO_2 on Al_2O_3 and 25% KOH/Al_2O_3 catalysts.

The result shows desorption peaks of Al_2O_3 and 25% KOH/Al_2O_3 at 155°C and 195°C, respectively. The temperature of ~155°C can be attributed to the interaction of CO_2 with sites of weak basic strength (Yin *et al.*, 2004). It has been proposed that these sites correspond to the OH^- groups on the surface. A desorption peak for 25% KOH/Al_2O_3 can be attributed to basic sites of medium strength, related to the activity of that catalyst (Xie *et al.*, 2006). It is clearly observed that the basic strength increases as the KOH loading increases.

4.2.4.2 KOH/NaY catalysts

The TPD profiles of desorbed CO_2 on NaY and KOH/NaY are shown in Figure 4.9.

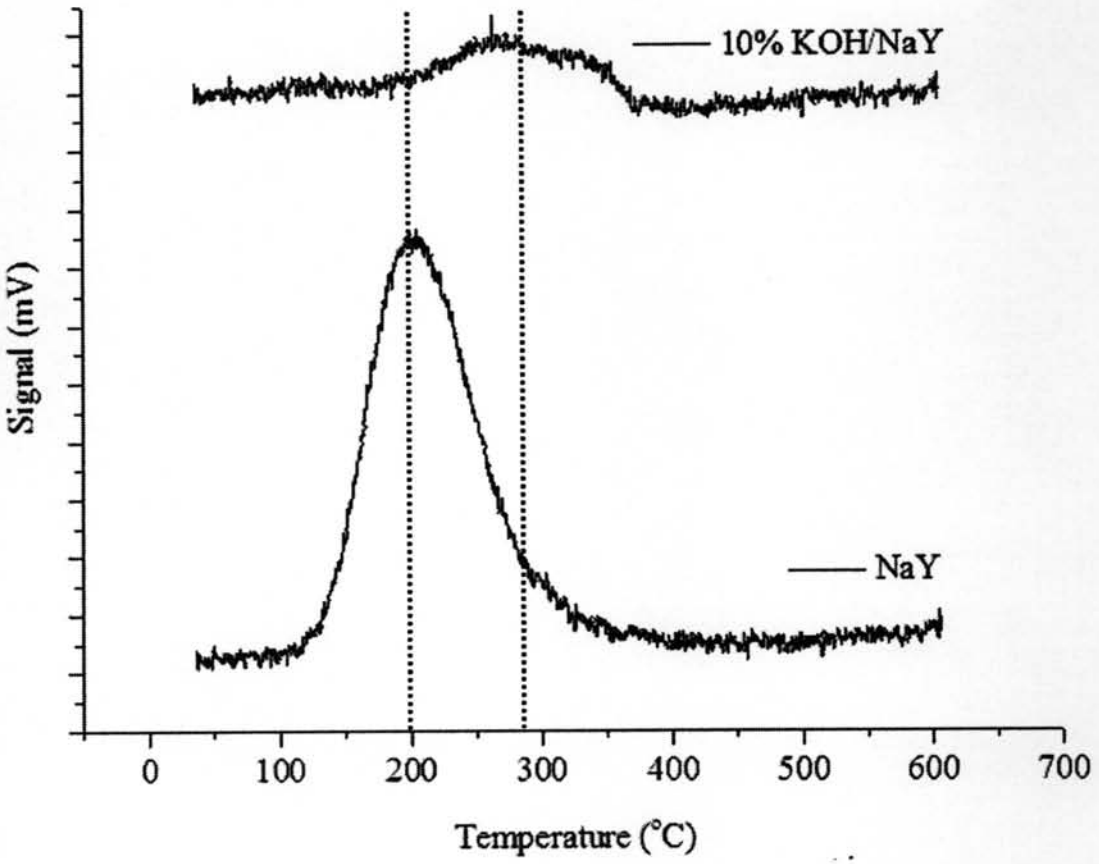

Figure 4.9 TPD profiles of CO_2 on NaY and 10% KOH/NaY catalysts.

Similarly, the result shows desorption peaks of NaY and 10% KOH/NaY at 200°C and 285°C, respectively. The temperature of 200°C can be attributed to the interaction of CO_2 with sites of weak basic strength (Yin *et al.*, 2004). It has been proposed that these sites correspond to the OH^- groups on the surface. A desorption peak for 10% KOH/NaY can be attributed to basic sites of medium strength, related to the activity of that catalyst (Xie *et al.*, 2006). It is clearly observed that the basic strength increases as the KOH loading increases.

4.3 Heterogeneous Catalytic Transesterification of Palm Oil

Based on the molecular weight of palm oil, the mass balance from the trans-esterification with methanol can be written as follows:

100 g Palm Oil + 11.29 g Methanol ➔ 100.47 Methyl Ester + 10.82 g Glycerol.

From the stoichiometry of the transesterification, the reaction requires 1 mole of vegetable oil and 3 moles of alcohol to form 3 moles of methyl ester and 1 mole of glycerol. Consequently, based on the molecular weight of the palm oil used in this work, 100 g of palm oil requires 11.29 g of methanol to complete the reaction.

In general, the reaction is conducted close to the boiling point of methanol (60°C to 70°C) at atmospheric pressure. Therefore, the reaction temperature used in this experiment was fixed at 60°C and the reaction time used was as long as possible to give the highest yield of biodiesel.

After the transesterification of triglycerides, the products are a mixture of esters, glycerol, spent solid catalyst, methanol, monoglyceride, diglyceride and triglyceride. The spent catalyst is separated from the product mixture by filtration. Afterward, the product mixture is placed in a separatory funnel and allowed to stand overnight to ensure that the separation of the methyl esters and the glycerol phase occur completely. The glycerol phase (bottom phase) is removed and left in a separate container. The methyl esters (top phase) are washed with warm distilled water (50°C) until the wash-water is clear. Finally, the methyl esters (biodiesel) are dried by adding 25wt% base on weight of the methyl esters product.

Unavoidable and undesirable reactions would, however, occur to form soap. This can be observed from the characterization of vegetable oil. The presence of water and free fatty acid in the vegetable oil forces the formation of soap. These reactions are shown in Figure 4.2.

$$RCOOR' + H_2O \rightleftharpoons \text{Free Fatty Acid} + R'OH$$

$$\text{Free Fatty Acid} + \text{Alkali} \rightleftharpoons \text{Soap} + H_2O$$

Figure 4.10 Hydrolysis and saponification reaction.

4.4 Transesterification reaction

KOH/Al_2O_3 and KOH/NaY zeolite catalysts were classified as basic and studied as a heterogeneous catalyst for transesterification. To investigate the optimum conditions for these catalysts on the transesterification of palm oil, the starting conditions for the potassium hydroxide on the alumina support was set with 20% KOH/Al_2O_3 at a methanol:oil molar ratio of 15:1, 3 wt% of the catalyst (based on the weight of the vegetable oil), a reaction temperature of 60°C, and a stirrer speed of 300 rpm . The starting conditions for the potassium hydroxide on the NaY support was set with 10% KOH/NaY at a methanol:oil molar ratio of 15:1, 6 wt% of catalyst (based on the weight of the vegetable oil), a reaction temperature of 60°C, and a stirrer speed of 300 rpm.

4.4.1 Influence of reaction time on the biodiesel yield

The effect of reaction time on the yield of biodiesel was studied using the 20% KOH/Al_2O_3 catalyst at molar ratio of methanol/oil at 15:1, 3 g of the catalyst, 300 rpm stirrer speed, and 60°C; and the 10% KOH/NaY catalyst at 15:1 methanol/oil molar ratio, 6 g of the catalyst, 300 rpm of stirrer speed, and 60°C. The reaction time was varied within a range from 1 to 6 hours. As can be seen from Figure 4.11, for the KOH/Al_2O_3 catalyst, the yield increased in the initial 2 hours and afterwards remained nearly constant as a result of near-equilibrium conversion. A maximum yield of 87.5% was obtained after 6 hours. The optimum reaction time was obtained at 2 hours where the yield of biodiesel was about 81.96%. Similarly, for the KOH/NaY catalyst, the yield increased in 2-3 hours and afterwards remained nearly constant. The optimum reaction time was obtained at 3 hours and the yield of biodiesel was about 91.07%. (The composition of biodiesel with various reaction

times is presented in Appendix C, table C1 and C2. It shows that the composition of the biodiesel remained almost constant when varying the reaction time.)

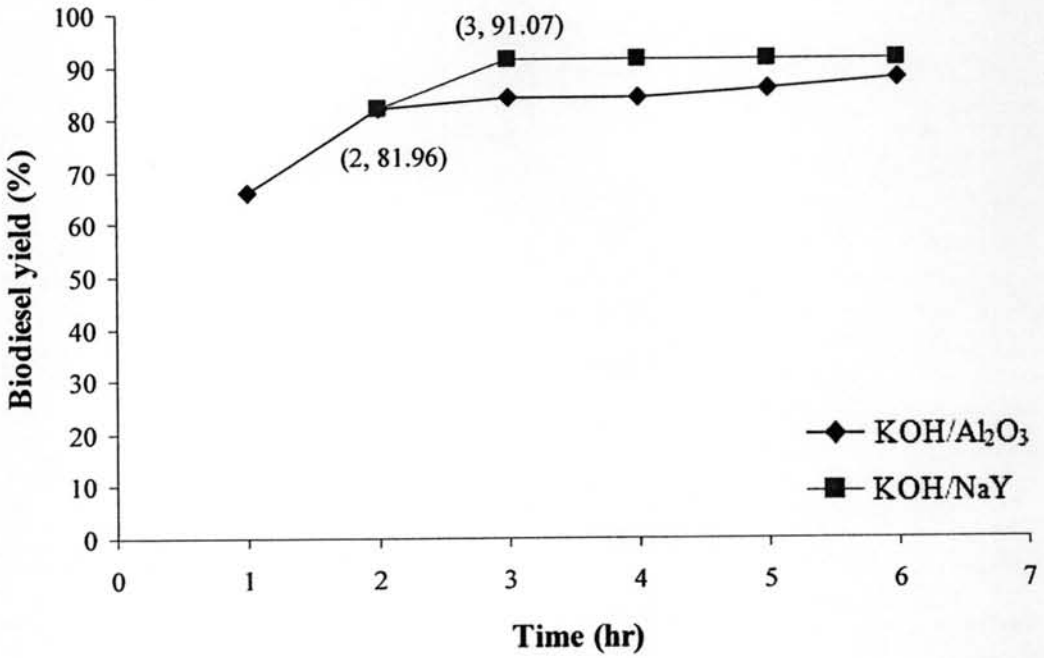

Figure 4.11 Yield of biodiesel as a function of reaction time.

4.4.2 Influence of wt% of potassium hydroxide loading on the biodiesel yield

The effect of wt% KOH loading on the yield of biodiesel was studied. The KOH/Al_2O_3 catalysts were prepared by varying the loading amount of KOH from 5 to 35 wt% and were used to catalyze the transesterification reaction. Reaction conditions for the KOH/Al_2O_3 was 2 hours reaction time, 15:1 methanol/oil molar ratio, 3 g catalyst amount, 300 rpm stirrer speed, and 60°C. The results are shown in Figure 4.12. The results revealed that as the loading amount of KOH was increased from 15 to 25 wt%, the biodiesel yield was increased, and the highest yield (91.07%) was obtained at a KOH loading of 25 wt% on Al_2O_3. However, when the amount of loaded KOH was over 25 wt%, the biodiesel yield decreased. It is believed that the agglomeration of the active KOH phase or the covering of the basic sites by the excess KOH occurred, and hence a lowering of the surface area of the catalyst and

lower activity. These results agree well with the result from the XRD patterns and the previous work on KNO_3/Al_2O_3 reported by Xie *et al.* (2006). They explained that the new phase of K_2O was the cause of the high catalytic activity and basicity of the catalyst since, when increasing the KOH loading to 15-25 wt%, the new phase of K_2O was observed and the biodiesel yield was increased. And when further increasing the KOH loading over 25 wt%, a new phase of Al-O-K compound was observed and the biodiesel yield decreased. This is because the new phase (Al-O-K) compound has lower catalytic activity and basicity than the K_2O phase. Correspondingly, the KOH/NaY catalysts were prepared by varying the loading amount of KOH from 8 to 15 wt% and were used to catalyze the transesterification reaction. The reaction conditions for KOH/NaY was 3 hours of reaction time, 15:1 methanol/oil molar ratio, 6 g of catalyst amount, 300 rpm of stirrer speed, and 60°C. The results showed that as the loading amount of KOH was increased from 8 to 10 wt%, the biodiesel yield was increased, and the highest yield (91.07%) was obtained at a KOH loading of 10 wt% on NaY. When the amount of loaded KOH was over 10 wt%, the biodiesel yield was decreased.

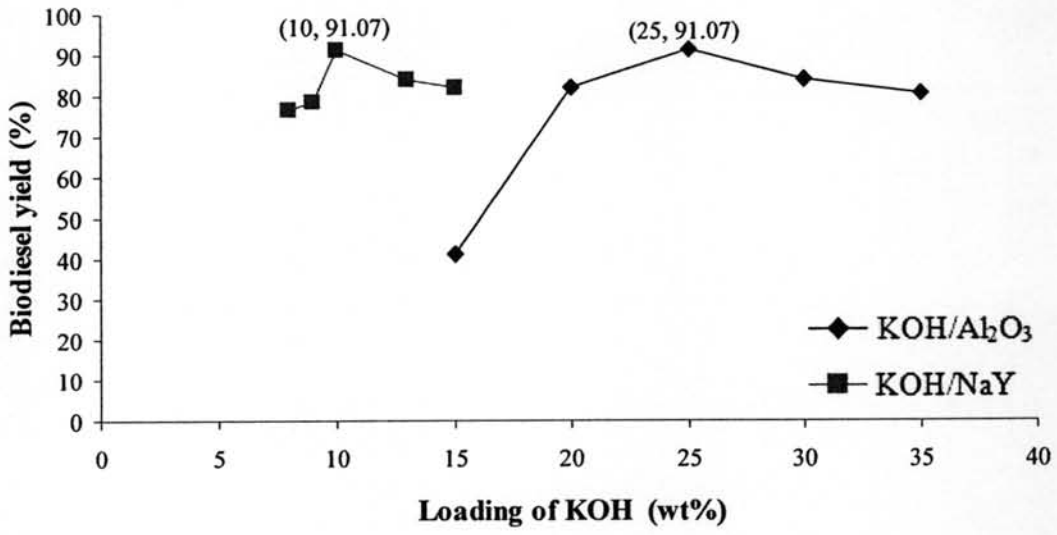

Figure 4.12 Yield of biodiesel as a function of wt% KOH.

The composition of biodiesel with varying wt% of KOH loading are presented in Appendix C(3-4), which shows that the composition of the biodiesel is almost constant when varying the wt% of the KOH loading.

In addition, the product distribution in the esteric phase for the run performed at 60°C in the presence of KOH/Al_2O_3 and KOH/NaY catalysts was determined by GC analysis. The methyl ester content and mono-, di-, tri-glycerides of biodiesel with various wt% loadings of KOH on Al_2O_3 and NaY are shown in Figures 4.13 – 4.14, respectively. For KOH/Al_2O_3, methyl ester content was increased when the loading amount of KOH was increased from 15 to 25 wt% and the highest methyl ester content of 95.48 %w/w was obtained at a KOH loading of 25 wt% on Al_2O_3. But mono-, di- and tri-glycerides decreased when increasing the KOH loading since the transesterification consists of a sequence of three consecutive and reversible reactions. In the first step, tri-glyceride is converted to diglyceride. In the second, diglyceride is converted to monoglyceride, and then monoglyceride is converted to glycerol. For each step, one molecule of methyl ester is liberated, so when the methyl ester increased, the mono-, di- and tri-glycerides were decreased because these three types of glyceride are converted to methyl ester.

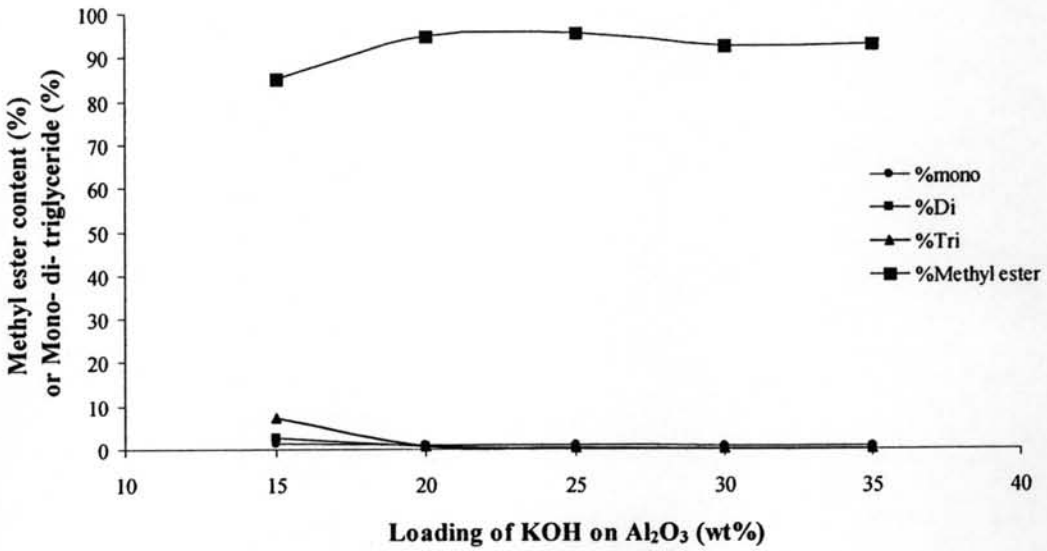

Figure 4.13 Methyl ester content and mono-, di-, triglycerides of biodiesel as a function of wt.% KOH loading on alumina.

In the same way, for the KOH/NaY catalyst, it was shown that methyl ester content was increased when the loading amount of KOH was increased from 8 to 13 wt%, and the highest methyl ester content of 92.84 %w/w was obtained at a KOH loading of 13 wt% on NaY.

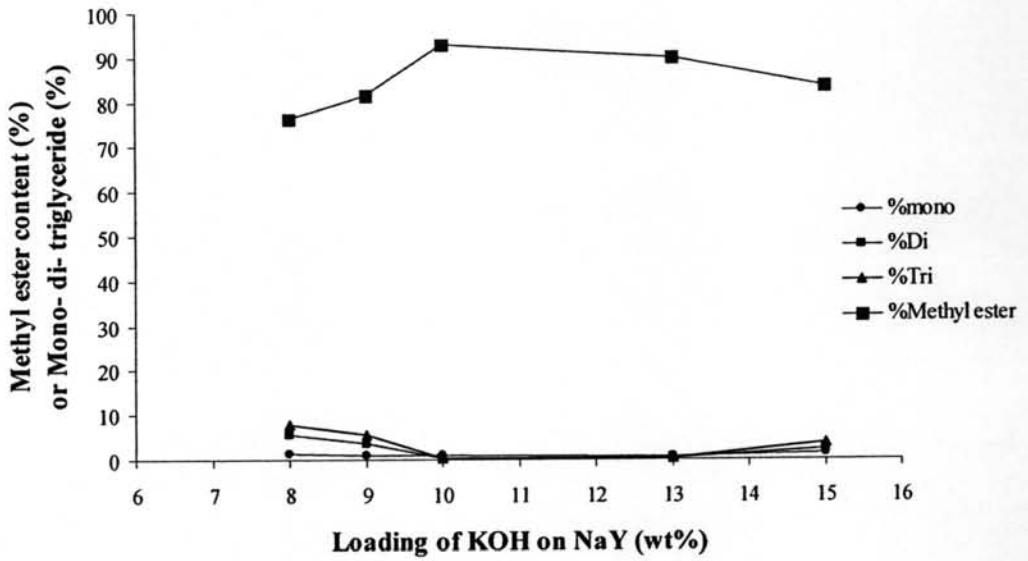

Figure 4.14 Methyl ester content and mono-, di-, triglycerides of biodiesel as a function of wt.% KOH loading on NaY.

The conversions of biodiesel with various wt% loadings of KOH on Al_2O_3 and NaY are shown in Figure 4.15. For the KOH/Al_2O_3 catalyst, it is shown that the highest conversion (86.93%) was obtained at a KOH loading of 25 wt% on Al_2O_3. And for the KOH/NaY catalyst, that the highest conversion (84.55%) was obtained at a KOH loading of 13 wt% on NaY.

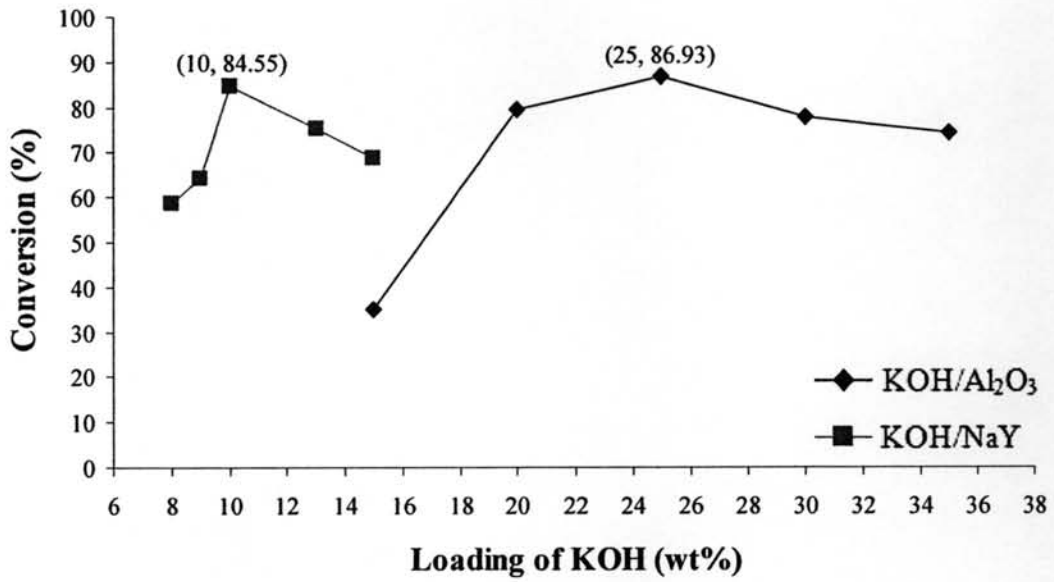

Figure 4.15 Conversion of biodiesel as a function of wt.% KOH loading.

4.4.3 Influence of molar ratio of methanol to oil on the biodiesel yield

From the stoichiometry, transesterification requires a molar ratio of methanol to oil of 3:1. Since this reaction is a reversible reaction, the effect of this molar ratio on the yield of methyl ester was studied by varying the methanol from 6 to 21. In addition, for the transesterification catalyzed by using a heterogeneous catalyst, mass transfer is limited, leading to low biodiesel yield, as shown in Figure 4.16. The reaction conditions for the KOH/Al_2O_3 were 2 hours reaction time, 25 wt% KOH, 3 g of catalyst amount, 300 rpm of stirrer speed, and 60°C. The results showed that when the molar ratio of methanol to oil was increased, the biodiesel yield was increased and the highest yield (91.07%) was obtained at a molar ratio of methanol to oil of 15:1. Beyond the molar ratio of 15:1, the excess amount of methanol had no effect on biodiesel yield. However, it has been reported that when amount of methanol was over 15:1, glycerol separation become more difficult, resulting in a decrease of biodiesel yield (Kim *et al.*, 2004). For the KOH/NaY catalyst, reaction conditions were 3 hours reaction time, 10wt% KOH, 6 g of catalyst, 300 rpm of stirrer speed, and 60°C. The result showed that when the molar ratio of methanol to oil was increased, the biodiesel yield increased and the highest yield (91.07%) was obtained at a molar ratio of methanol to oil of 15:1. When further increasing the molar ratio of

methanol to oil over 15:1, the excess amount of methanol had no effect on biodiesel yield. The composition of biodiesel with various molar ratios of methanol to oil are presented in Appendix C(5-6) which show that the composition of biodiesel was almost constant.

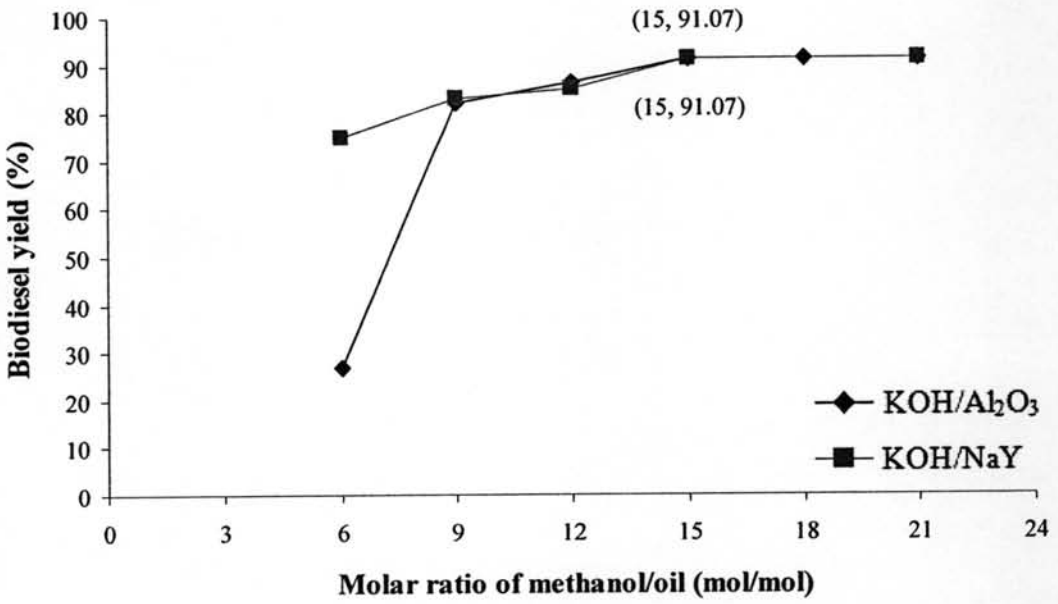

Figure 4.16 Yield of biodiesel as a function of molar ratio of methanol to oil.

4.4.4 Influence of amount of catalyst on the biodiesel yield

To determine the influence of amount of catalyst on biodiesel yield, the catalyst amount was varied within the range of 1-5 wt%. The reaction was carried out with 25 wt% KOH/Al_2O_3 at a methanol/oil molar ratio of 15:1, stirrer speed of 300 rpm, and temperature of 60°C. The results showed that when the amount of catalyst was not sufficient, the yields of biodiesel are relatively low (~80%). Biodiesel yields were increased from 80.35% to 91.07% as the amount of KOH/Al_2O_3 increased from 1 to 3 g. And with a further increase in the amount of catalyst over 3 g, the mixture of reactants and catalyst became too viscous, leading to a problem of mixing. To avoid these problems, the optimum condition must be employed at 3 g, which gave a 91.07% yield of biodiesel. The reaction with the KOH/NaY catalyst was carried out with 10 wt% KOH/NaY at a methanol/oil molar

ratio of 15:1, 300 rpm stirrer speed, and 60°C. The results showed that at low amounts of catalyst, the yields of biodiesel are relatively low (~73%). With a further increase in the amount of catalyst, the biodiesel yields increased from 73.21% to 91.07%. The optimum amount of catalyst was 6 g, and 91.07% yield of biodiesel was obtained, as shown Figure 4.17. In addition, the composition of biodiesel with various amount of catalysts are presented in Appendix C(7-8) which show that the composition of biodiesel was almost constant.

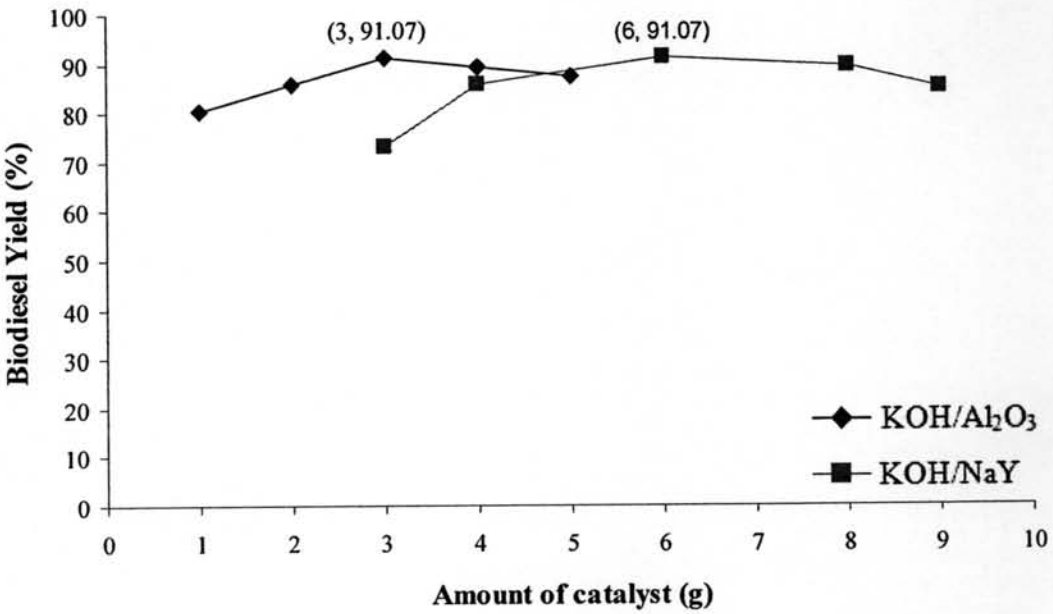

Figure 4.17 Yield of biodiesel as a function of amount of catalyst.

4.4.5 Influence of reaction temperature on the biodiesel yield

The reaction temperature of transesterification was investigated in a range from 30 to 70°C. The results shown in Figure 4.18 indicate that at low reaction temperature (room temperature), the yields of biodiesel are relatively low (75%) after 2 hours of reaction. The biodiesel yield increased (to ~95%) with an increase of reaction temperature to 70°C. The optimum reaction temperature was considered to be around 60°C, which does not exceed the boiling point of methanol. The composition of biodiesel with various reaction temperatures are presented in Appendix C9. The

result showed that the composition of biodiesel was not changed when the reaction temperature was changed.

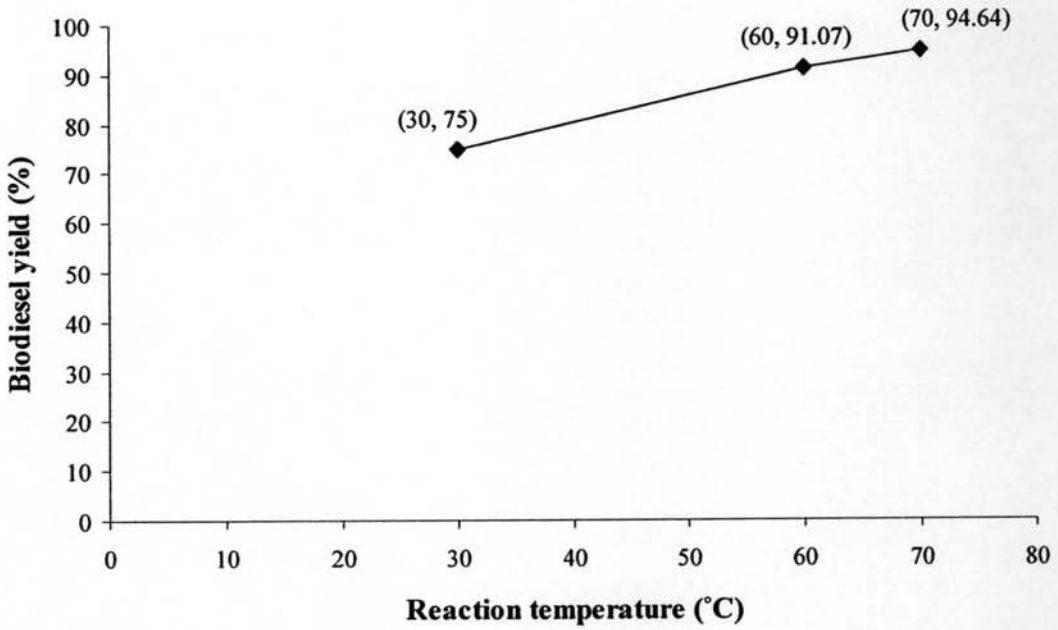

Figure 4.18 Yield of biodiesel as a function of reaction temperature. Reaction conditions: reaction time, 2 hours; 25 wt% KOH/Al_2O_3; methanol/oil molar ratio, 9:1; stirrer speed, 300 rpm.

4.4.6 Influence of stirrer speed on the biodiesel yield

The stirrer speed was studied in the range of 150 – 600 rpm. The results showed that the stirrer speed had almost no effect on the product yield, as shown in Figure 4.19. A maximum yield of 92.85% was obtained at a stirrer speed of 600 rpm. The optimum stirrer speed was obtained at 300 rpm. The result is in agreement with the result of a heterogeneous base catalyst reported by Kim *et al.*, the composition of biodiesel with various stirrer speeds are presented in Appendix C10, which shows that the composition of biodiesel was almost constant when varying stirrer speed.

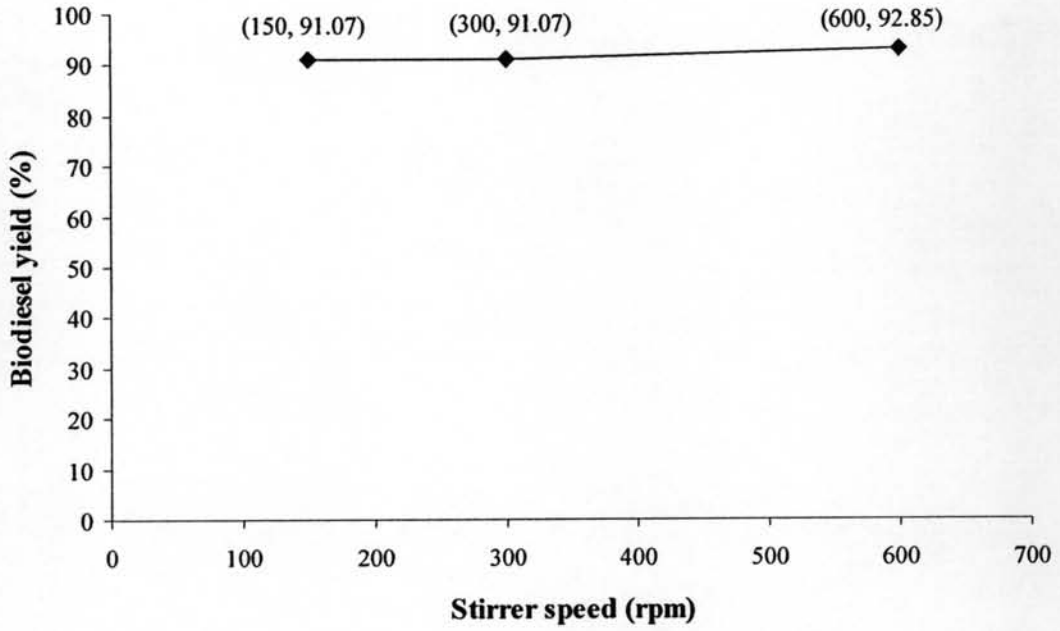

Figure 4.19 Yield of biodiesel as a function of stirrer speed. Reaction conditions: reaction time, 2 hours; 25 wt% KOH/Al_2O_3; methanol/oil molar ratio, 9:1; temperature, 60°C.